

# Spin Dynamics of Strongly Correlated Systems

B. Keimer, Max-Planck-Institute for Solid State Research  
70669 Stuttgart, Germany

## 1. Introduction

In introductory physics classes, we are taught that solids are described by band theory. As a starting point, one takes the kinetic energy of the electrons and their Coulomb interactions with the regular array of nuclei into account, but neglects the mutual Coulomb repulsion between the electrons. Does this make any sense? It is clear that the reasons for the validity of this approximation have to be subtle, because the latter energy scale is of course of the same order of magnitude as the former two. It can, however, be justified on the basis of the so-called Fermi liquid theory: Under certain quite general conditions, the electron eigenstates of an interacting electron system can be adiabatically transformed into those of a noninteracting system. There is no doubt that Fermi liquid theory provides an excellent description of simple three-dimensional metals and semiconductors; this is why it is taught in school.

But there are also some well-known cases in which Fermi liquid theory breaks down: A one-dimensional metal, for instance, is theoretically described by the so-called Tomonaga-Luttinger theory that bears little resemblance to a noninteracting electron gas, no matter how weak the interactions. In particular, there is no sharp "Fermi edge" that separates occupied and unoccupied states (even at zero temperature). Unfortunately, one-dimensional metals are extremely difficult to realize in nature, because quasi-one dimensional electron systems in real materials are subject to so-called Peierls instabilities in which the lattice spontaneously distorts and transforms the system into a band insulator. Although it costs energy to distort the lattice, it can be shown that this is outweighed by the lowering of the electronic ground state energy due to the introduction of the band gap. Even a one-dimensional metal on a rigid lattice is unstable against the formation of a so-called spin density wave, a magnetically ordered state that induces band gaps through a spin-dependent potential.

If the effective electron-electron interaction is sufficiently strong, insulating states can also replace the Fermi liquid in higher dimensional systems that ought to be metallic according to band theory. This happens in materials involving *d*- and *f*-electrons that are tightly bound to the atomic core, so that they are forced to spend a lot of time together. Especially in cases in which there is an integer number of such electrons per atom, these often prefer to localize at a particular atom and thereby give up some quantum-mechanical kinetic energy, rather than forming a Fermi liquid and being subject to perpetual collisions with other electrons.

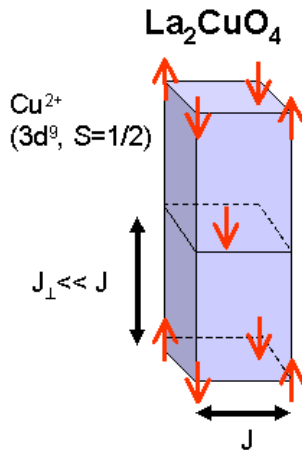


**Fig. 1:** Magnetic structure of insulating La<sub>2</sub>CuO<sub>4</sub>.

The result is the well-known "Mott insulator", realized in simple members of many material systems that will be of interest later (Figure 1). *Charge* excitations in a Mott insulator require a high energy, because in the transfer of a localized electron from one atom to the next one has to overcome the large Coulomb repulsion of the electron localized on the neighboring atom. They are "frozen out", that is, the energy gap for charge excitations is much larger than typical temperatures. The *spin* degrees of freedom, on the other hand, give rise to low energy excitation modes termed "spin waves". They are described by the "spin Hamiltonian", often of the Heisenberg form

$$H = \sum_{ij} J_{ij} \underline{S}_i \cdot \underline{S}_j$$

The magnitude and the sign of the exchange parameters  $J_{ij}$  is determined the relative orientation of the orbitals of neighboring magnetic atoms (*d*-orbitals in the case of La<sub>2</sub>CuO<sub>4</sub> shown in Figure 1). This is described in Section 4 below. Here we regard them simply as fixed parameters. Since  $J_{ij}$  falls off rapidly with increasing separation of the atoms *i* and *j*, it is usually a good approximation to consider nearest-neighbor interactions only. It is then straightforward to derive the excitation spectrum of *H*. For the two-dimensional square lattice (appropriate for La<sub>2</sub>CuO<sub>4</sub> because of its layered structure, see Fig. 1), one obtains

$$\hbar\omega = 4SJ\sqrt{1 - \gamma^2(\underline{q})}$$

where  $\gamma(\underline{q}) = \frac{1}{2}[\cos(q_x a) + \cos(q_y a)]$  and *a* is the nearest-neighbor distance. This is the dispersion relation of a spin wave. Cartoons in both real space and reciprocal space are shown in Figure 2.

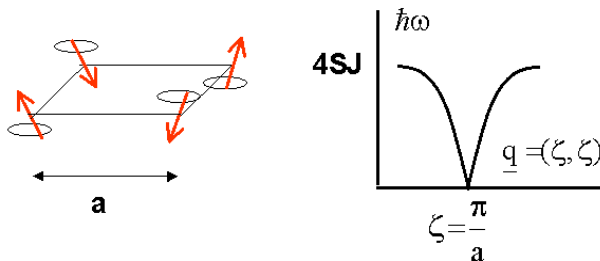


**Fig. 2:** Schematic representation of a spin wave for a two-dimensional square lattice with nearest-neighbor exchange interaction *J* and spin *S*.

Since the typical energy scale for **J** is 1-100 meV, spin waves can be readily detected by inelastic scattering of thermal neutrons. Through the fluctuation-dissipation theorem

$$\frac{\partial^2 \sigma}{\partial \Omega \partial \omega} \propto [1 - e(-\hbar\omega / k_B T)]^{-1} \chi''(\underline{q}, \omega)$$

the neutron cross section is proportional to the imaginary part,  $\chi''(\underline{q}, \omega)$ , of the wave vector and energy dependent dynamical susceptibility  $\chi(\underline{q}, \omega)$ , which describes the response of the magnetization  $\mathbf{M}$  to a generalized magnetic field:

$$M(\underline{q}, t) = \chi H(\underline{q}) \exp(-i\omega t)$$

Here, as in the following, we do not worry too much about constants of proportionality that can be looked up in textbooks, and focus on the essential physics. In the case of scattering from spin waves, the dynamical susceptibility is given by a delta-function

$$\chi''(\underline{q}, \omega) = \pi (g\mu_B)^2 \delta(\hbar\omega - \hbar\omega(\underline{q}))$$

that is nonzero only for points along this dispersion relation. The constant of proportionality is chosen such that in the limit  $\underline{q} = \omega = 0$  the definition is compatible with that of the uniform susceptibility whose real part,  $\chi'(0,0)$ , is measured in a standard magnetization experiment. It will henceforth be omitted for clarity.

Spin waves in Mott insulators, where the effective Coulomb interactions are so strong that all electrons are localized, have been studied for many years, and the physics is well understood. In the opposite limit, that of a noninteracting gas of electrons, the spin excitations are also, in principle, well understood. Low energy excitations (with excitation energy much smaller than the Fermi energy) are created by flipping the spin of an electron near the Fermi surface and propagating it to a different location in reciprocal space, as depicted in Figure 3.

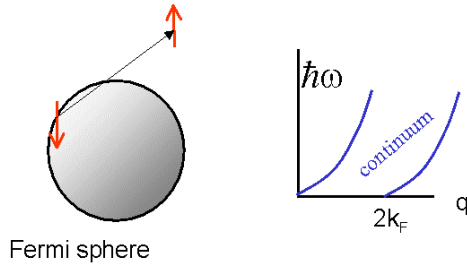


**Fig. 3:** Schematic representation of magnetic excitations in a noninteracting electron gas.

The excitation spectrum forms a broad continuum, because spin-flip excitations with the same energy can have many different wave vectors. For instance, zero energy excitations can be created with wave vectors  $0 < q < 2k_F$ . From Fermi's Golden Rule, we know that the cross section (and hence the dynamical susceptibility) can be written as

$$\chi_0''(\underline{q}, \omega) = \pi \sum_{\mathbf{k}} [f(E_{\mathbf{k}+\mathbf{q}\uparrow}) - f(E_{\mathbf{k}\downarrow})] \delta(E_{\mathbf{k}+\mathbf{q}} - E_{\mathbf{k}} - \hbar\omega).$$

where  $f$  is the Fermi function and the arrows indicate spin-up and spin-down states, respectively. Using the identity

$$\text{Im} \lim_{\varepsilon \rightarrow 0} (x + i\varepsilon)^{-1} = -\pi \delta(x),$$

this is also often written as

$$\chi_0(\underline{q}, \omega) = \sum_{\mathbf{k}} \frac{f(E_{\mathbf{k}+\mathbf{q}\uparrow}) - f(E_{\mathbf{k}\downarrow})}{\hbar\omega - (E_{\mathbf{k}+\mathbf{q}} - E_{\mathbf{k}}) + i\varepsilon}$$

where it is understood that  $\varepsilon \rightarrow 0$ . This should give a good description of the magnetic spectrum of a simple metal such as, say, Na. Unfortunately, the spectral weight of the continuum spin excitations is so weak that they have actually never been observed by inelastic neutron scattering.

In both of these limiting cases (very strong and very weak interactions, respectively) the magnetic dynamics of electrons is therefore well understood, at least in principle. Current interest has shifted to the intermediate case, where the effective electron-electron interactions are neither negligible nor strong enough to induce localization. This is the situation realized in "strongly correlated" metals such as high temperature superconductors that are being studied by many experimental groups around the world. Of interest are not only the physical origin of superconductivity, but also the more general question of whether the Fermi liquid theory is at all a valid starting point for a theoretical description. Do we have to completely reinvent the theory of metals, or can we get away with some minor patchwork? There are many indications that the former is the case, which makes this field so interesting, but this can ultimately only be established experimentally. Since the dynamical susceptibility  $\chi(\underline{q}, \omega)$  measured by neutron scattering yields incisive information about the electron-electron interactions on precisely the relevant energy and length scales, it is widely considered as one of the most important probes of these materials.

Before giving an overview of our present (incomplete) understanding of spin excitations in high temperature superconductors, we begin by briefly reviewing the magnetic dynamics of some weakly correlated metals where the theory is already rather advanced.

## 2. Weakly Correlated Metals

It is well known that ferromagnetism in solids is ultimately due to electron-electron interactions. Due to the Pauli principle, two electrons in a spin-triplet state (with nonzero total spin) have to be in a spatially antisymmetric state, so that their Coulomb repulsion is minimized. A qualitative model of ferromagnetic solids such as Fe or Ni can therefore be constructed by considering a repulsive potential for electrons with antiparallel spin. For simplicity, we assume that this potential is completely local, that is,  $V_{\uparrow\downarrow}(\underline{r}) \propto U\delta(\underline{r})$ . This is not as unrealistic as it may seem, because for *d*- and *f*-electrons the short-range, intra-atomic Coulomb interactions between electrons tend to be much stronger than the long-range part of the interaction. In a ferromagnetically ordered state with nonzero magnetization *M* (which has to be derived self-consistently), this potential leads to a  $\underline{k}$ -independent energy difference  $\Delta \propto UM$  between spin-up and spin-down electrons. The external wave vector dependent magnetic field in the above formula is enhanced by an internal term  $\propto UM(\underline{q})$ , so that the total susceptibility becomes

$$\chi(\underline{q}, \omega) = \frac{\chi_0(\underline{q}, \omega)}{1 - U\chi_0(\underline{q}, \omega)}$$

where

$$\chi_0(\underline{q}, \omega) = \sum_{\underline{k}} \frac{f(E_{\underline{k}+\underline{q}\uparrow}) - f(E_{\underline{k}\downarrow})}{\hbar\omega - (E_{\underline{k}+\underline{q}} - E_{\underline{k}} - \Delta) + i\varepsilon}$$

Again, we have omitted some constants to keep the formula simple. A full derivation can be found in textbooks. Several important results are apparent: The continuum is now gapped due to the splitting in spin-up and spin-down bands, and the susceptibility is *enhanced*. Further, the renormalized susceptibility now has *poles*, in addition to the continuum, that are determined by the condition that the denominator

of the imaginary part of  $\chi(\underline{q}, \omega)$  vanish. These poles correspond to true collective modes. The complete excitation spectrum is sketched in Figure 4 below.

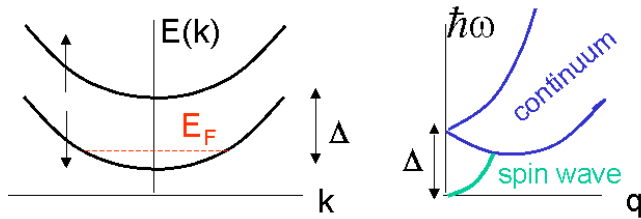


**Fig. 4:** Sketch of the spin-up and spin-down band dispersions and the spin excitation spectrum of a metallic ferromagnet.

The collective mode is readily interpreted as a spin wave, in analogy to the spin waves in Mott insulators discussed above. Their existence is a general consequence of the broken rotational symmetry in the magnetically ordered state, which always goes along with a so-called "Goldstone mode" whose energy approaches zero at the ordering wave vector ( $\underline{q} = (\pi/a, \pi/a)$  for the two-dimensional antiferromagnet above,  $\underline{q} = 0$  for a ferromagnet). These spin waves can and have been observed in Fe, Ni, and other ferromagnets by inelastic neutron scattering.

Other elemental metals (Cr and Mn) undergo transitions into so-called "spin density wave states". This can be understood in analogy to the Peierls instability of one-dimensional metals mentioned above. In fact, the Fermi surfaces of these metals

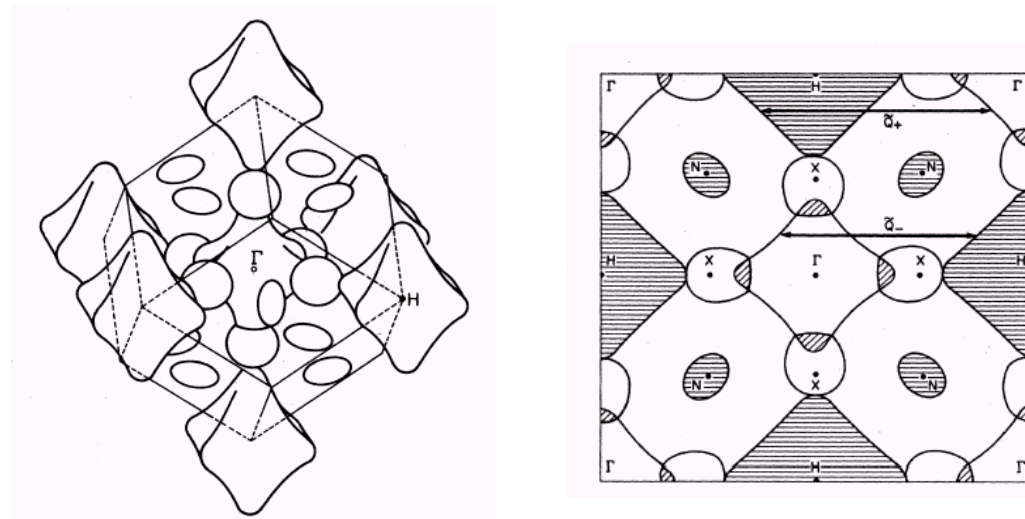
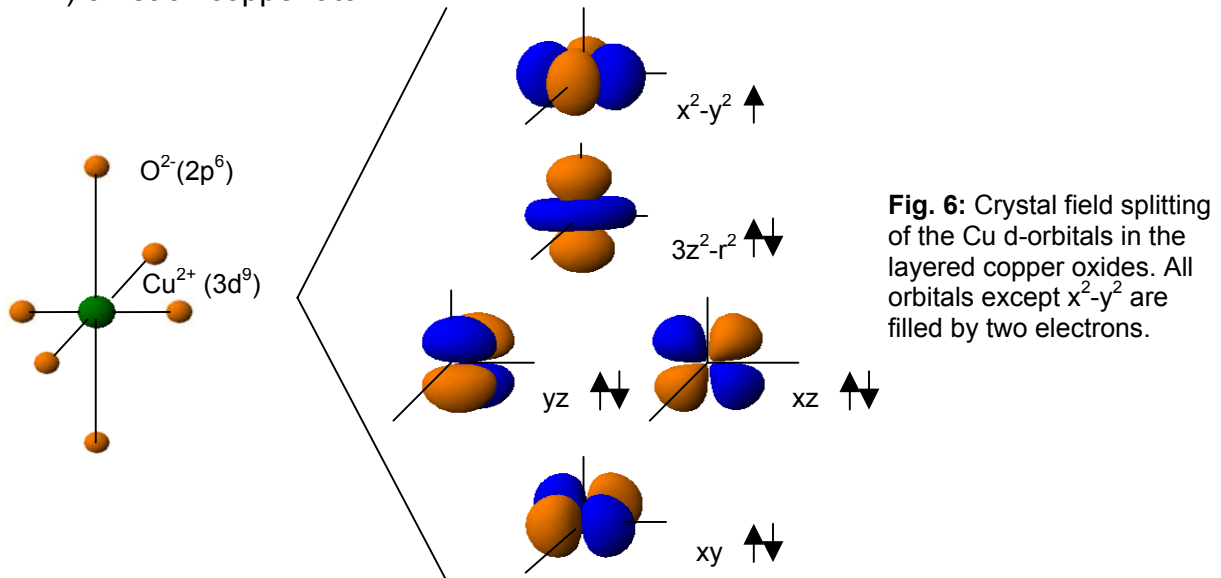


**Fig. 5:** Calculated Fermi surface of Cr and two-dimensional section showing typical nesting vectors [1].

satisfy the so-called "nesting condition", that is, large sections of their Fermi surfaces are parallel as sketched in Figure 5. As a consequence, the susceptibility resembles that of one-dimensional metals, and a magnetically ordered state with wave vector  $\underline{q}_0$  is stabilized if  $\chi_0(\underline{q}_0)$  exceeds a threshold value. Although the spin excitations in Cr and Mn are still the subject of active research, one does find well defined low energy spin waves around  $\underline{q} = \underline{q}_0$  as expected on general grounds.

### 3. High Temperature Superconductors

High temperature superconductivity was discovered in copper oxides in 1986. The many compounds that are now known to exhibit high temperature superconductivity share a single structural motif, the  $\text{CuO}_2$  layer, and electronic conduction is believed to be confined mostly to these layers. In the stoichiometric form (e.g.,  $\text{La}_2\text{CuO}_4$ , Fig. 1), simple valence counting shows that the electron configuration of Cu is  $3d^9$ , while that of O is  $2p^6$ . Oxygen is thus nonmagnetic, and there is a single hole (with spin  $1/2$ ) on each copper atom.



As indicated by the above crystal field level scheme, the hole resides in the  $x^2-y^2$   $d$ -orbital of Cu. The layered structure of the copper oxides results in a large crystal field splitting, so that the completely filled  $d$ -orbitals are irrelevant for the electronic structure. For undoped copper oxides, the Cu holes form a Mott insulating state with antiferromagnetic spin structure. Interesting physics begins to appear when additional holes are introduced into the  $\text{CuO}_2$  layers by chemical substitution (e.g., by replacing trivalent La by divalent Sr in  $\text{La}_{2-x}\text{Sr}_x\text{CuO}_4$ ). At a threshold concentration of additional holes ( $\sim 5\%$ ), the antiferromagnetic state is replaced by a metallic phase with unconventional physical properties (e.g.,  $T$ -linear resistivity over a very wide range of temperatures), and by a superconducting state at low temperatures, as shown in Fig. 7.

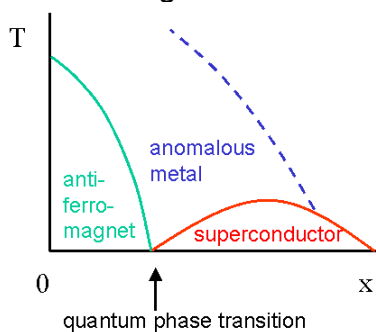


**Fig. 7:** Generic phase diagram of the copper oxide superconductors, as a function of the temperature ( $T$ ) and the hole concentration in the copper oxide layers that can be varied by changing the chemical composition (e.g.,  $x$  in  $\text{La}_{2-x}\text{Sr}_x\text{CuO}_4$  or  $\text{YBa}_2\text{Cu}_3\text{O}_{6+x}$ ).

A look at Fig. 7 convinces one that the copper oxides should be regarded as strongly correlated metals: The strong Coulomb interactions that give rise to the Mott insulating state will not simply disappear upon doping (that is, changing the parameter  $x$ ). This also immediately suggests a mechanism for high temperature superconductivity: If electronic interactions (whose energy scale extends up to several eV) are responsible for pairing the electrons, rather than phonons (whose energy scale is over the order of several meV, and which are known to be responsible for pairing and superconductivity in low temperature superconductors), then a high transition temperature comes naturally. Briefly said, "electrons pair themselves". As always, however, the devil is in the details: It has proven remarkably difficult to translate this simple physical intuition into a full theory. The reason is that our conventional understanding of metals (encapsulated in the Fermi liquid theory) is based on perturbations around the noninteracting limit and is therefore only of limited usefulness for this problem. Mapping out the spin excitations by neutron scattering gives essential guidance for new theories incorporating strong interactions from the beginning. Fortuitously, the superconducting energy gap in these systems is also of the same order as the energy of typical thermal neutrons.

While the efforts to explain the anomalous metallic and superconducting phases are still in their infancy, remarkably general predictions exist for the spin dynamics near the point where these meet with the antiferromagnetic phase in the phase diagram of Fig. 7. This is because theories originating in the 1970's have shown that near a phase transition, the properties of a system (including its dynamics) should only depend on certain very general features such as the number of components of the order parameter and the spatial dimensionality, and should thus be common to many superficially dissimilar systems. These predictions take a particularly simple form near  $T=0$  phase transitions whose character is dominated by quantum fluctuations (so-called quantum phase transition). For two-dimensional antiferromagnets, it has been shown that [2]

$$\chi(\underline{q}, \omega) \propto T^{-(2-\eta)/z} F\left(\frac{\underline{q} - \underline{Q}_{AF}}{T^{1/z}}, \frac{\hbar\omega}{k_B T}\right)$$

where  $\underline{Q}_{AF} = (\pi/a, \pi/a)$  is the antiferromagnetic ordering wave vector,  $z$  is the so-called "dynamical critical exponent", and  $F$  is a scaling function to be determined by a detailed calculation. This means that a single characteristic length scale and a single characteristic energy scale determine the entire dynamics of the system, both of which are set by the temperature. In order to focus on one of these aspects, we can integrate over  $\underline{q}$  and consider the so-called local susceptibility  $\int d^2q \chi(\underline{q}, \omega)$ . This is plotted in Fig. 8 for  $\text{La}_{1.96}\text{Sr}_{0.04}\text{CuO}_4$ , a composition very close to the quantum critical point. The result shows that the spin susceptibility is indeed homogeneous in  $\omega/T$ , as predicted by the theory of quantum phase transitions. Very similar behavior has recently been observed near the quantum critical point of a "heavy fermion" system (with very different chemical composition and lattice structure) near a quantum critical point, confirming the "universality" of the temperature scaling observed in the copper oxides.

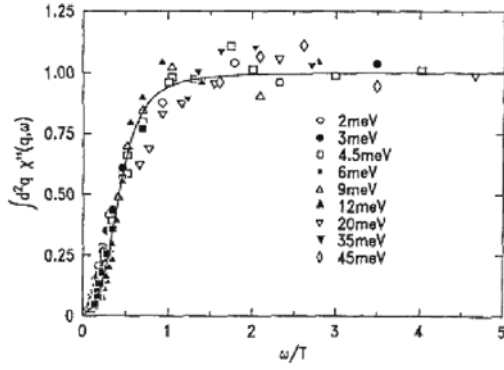


**Fig. 8:** Local susceptibility of  $\text{La}_{1.96}\text{Sr}_{0.04}\text{CuO}_4$ , near the quantum phase transition that separates antiferromagnetic and superconducting phases, as a function of the reduced parameter  $\omega/T$ . (Here:  $\hbar = k_B = 1$ .) [3]

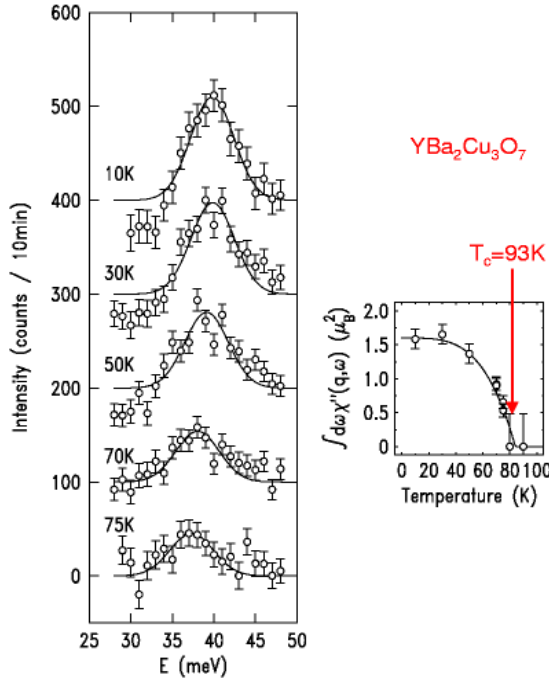


**Fig. 9:** Dynamical spin susceptibility of the high temperature superconductor  $\text{YBa}_2\text{Cu}_3\text{O}_7$  at the wave vector  $Q_{AF} = (\pi/a, \pi/a)$ .  $T_c$  is the superconducting transition temperature [4].

At larger hole concentrations,  $\text{La}_{2-x}\text{Sr}_x\text{CuO}_4$  becomes superconducting. In the superconducting state, pronounced spin excitations can still be observed, with wave vector at or close to the antiferromagnetic ordering wave vector. The spin excitation spectrum is strongly changed upon entering the superconducting state, which gives credence to our assumption above that some electronic excitation stabilizes superconductivity. A particularly striking example is the so-called "resonance peak" whose properties are summarized in Fig. 9.

The spectral weight of this sharp excitation is concentrated around the wave vector  $(\pi/a, \pi/a)$  and is nonzero only in the superconducting state. Below  $T_c$ , it follows an order-parameter-like behavior. How do we understand this unusual excitation? We can begin by writing down the dynamical susceptibility of an electron system described by a BCS wave function, but otherwise noninteracting [5]:

$$\chi_0(\mathbf{q}, \omega) = \sum_{\mathbf{k}} \left\{ \frac{1}{2} \left( 1 + \frac{\varepsilon_{\mathbf{k}} \varepsilon_{\mathbf{k}+\mathbf{q}} + \Delta_{\mathbf{k}} \Delta_{\mathbf{k}+\mathbf{q}}}{E_{\mathbf{k}} E_{\mathbf{k}+\mathbf{q}}} \right) \frac{f(E_{\mathbf{k}+\mathbf{q}}) - f(E_{\mathbf{k}})}{\omega - (E_{\mathbf{k}+\mathbf{q}} - E_{\mathbf{k}}) + i\delta} + \frac{1}{4} \left( 1 - \frac{\varepsilon_{\mathbf{k}} \varepsilon_{\mathbf{k}+\mathbf{q}} + \Delta_{\mathbf{k}} \Delta_{\mathbf{k}+\mathbf{q}}}{E_{\mathbf{k}} E_{\mathbf{k}+\mathbf{q}}} \right) \frac{1 - f(E_{\mathbf{k}+\mathbf{q}}) - f(E_{\mathbf{k}})}{\omega + (E_{\mathbf{k}+\mathbf{q}} + E_{\mathbf{k}}) + i\delta} \right. \\ \left. + \frac{1}{4} \left( 1 - \frac{\varepsilon_{\mathbf{k}} \varepsilon_{\mathbf{k}+\mathbf{q}} + \Delta_{\mathbf{k}} \Delta_{\mathbf{k}+\mathbf{q}}}{E_{\mathbf{k}} E_{\mathbf{k}+\mathbf{q}}} \right) \frac{f(E_{\mathbf{k}+\mathbf{q}}) + f(E_{\mathbf{k}}) - 1}{\omega - (E_{\mathbf{k}+\mathbf{q}} + E_{\mathbf{k}}) + i\delta} \right\}$$

where  $\delta \rightarrow 0$ ,  $\varepsilon_k$  are the band dispersions measured from the Fermi surface,  $\Delta_k$  is the superconducting energy gap function (whose magnitude and even sign is in general also  $k$ -dependent, depending on the internal structure of a Cooper pair), and

$E_k = \sqrt{\varepsilon_k^2 + \Delta_k^2}$ . The first term describes scattering of thermally excited electrons, completely analogous to the continuum excitations of a free electron gas discussed above, but now in the presence of the superconducting gap. The second and third terms describe annihilation and creation, respectively, of a spin-triplet pair of free electrons from a spin-singlet Cooper pair.

At low temperatures, where thermal energies are small but the resonance peak is most pronounced, the first two processes are negligible and only the third process, pair creation, is relevant. Looking at the susceptibility for this process, we notice two factors: The second factor is again a density-of-states factor of the form already encountered. The first factor is called "coherence factor", and it is a consequence of the functional form of the BCS wave function. Setting  $\varepsilon_k = 0$  (for excitation energies small compared to the Fermi energy), and plugging in the expression for  $E_k$  we notice that the coherence factor is **zero** if the gap function,  $\Delta_k$ , is isotropic ( $\Delta_k = \Delta_{k+q}$  for all  $\underline{k}$  and  $\underline{q}$ ), and the cross section for pair creation therefore vanishes. This is the reason why pair creation by magnetic neutron scattering has not been observed in ordinary superconductors. In the copper oxides, however, the gap function  $\Delta_k$  is highly anisotropic and even carries an unconventional  $d$ -wave symmetry. This is ultimately due to the strong Coulomb repulsion between the electrons: In order to minimize their relative separation, the electrons are bound up in a spin-singlet state with relative orbital angular momentum 2. (This guarantees the antisymmetry of the state as required by the Pauli principle. Recently, spin-triplet superconductivity with  $p$ -wave symmetry was discovered in another transition metal oxide,  $\text{Sr}_2\text{RuO}_4$ , but only below  $T=1.5\text{K}$ .)

Looking again at the cross section for pair creation, we notice that it is generally nonzero if  $\Delta_k$  has  $d$ -wave symmetry, as observed in the cuprates. In particular,  $\Delta_k = -\Delta_{k+q}$  for  $\underline{k} = (\pi/a, 0)$ ,  $\underline{q} = (\pi/a, \pi/a)$ . This alone is, however, not sufficient to explain the neutron data, because the resonance peak is very sharp in both energy and momentum while the continuum excitations described by  $\chi_0$  are always broad. In order to fully describe the data, it is necessary to introduce a  $\underline{q}$ -dependent generalization  $J(\underline{q})$  of the simple interaction potential used above for ferromagnetic metals:

$$\chi(\underline{q}, \omega) = \frac{\chi_0(\underline{q}, \omega)}{1 - J(\underline{q})\chi_0(\underline{q}, \omega)}$$

In analogy to the susceptibility of ferromagnetic metals discussed above, this expression can also have poles corresponding to collective modes. By fitting the neutron data, which are now available for a variety of different copper oxide compounds and doping concentrations, one can extract much useful information about the function  $J(\underline{q})$ , and thus about the electronic interactions that ultimately drive high temperature superconductivity. As already indicated by the proximity to the antiferromagnetic instability,  $J(\underline{q})$  is peaked at  $Q_{AF}$ . A detailed calculation yields a magnetic spectrum of the following form:

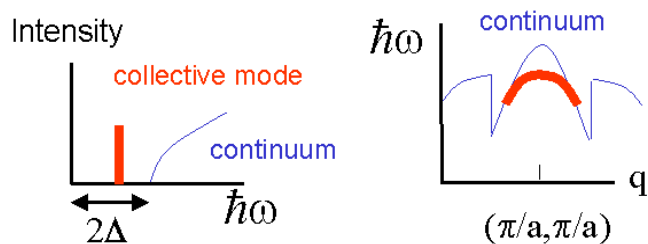
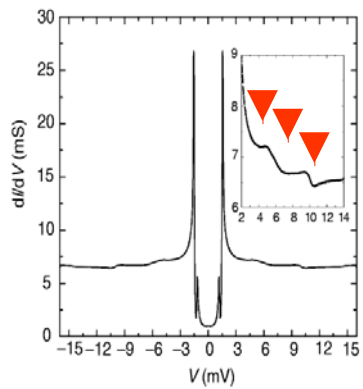


**Fig. 10:** Theoretical description of the experimentally observed resonant spin excitation mode.

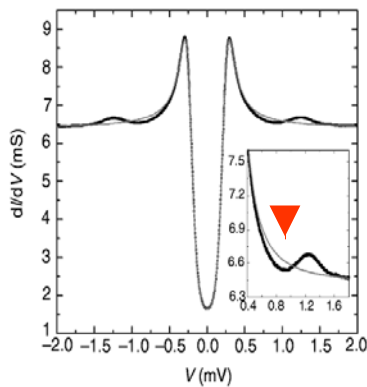
The downward dispersion sketched here has actually been observed recently [6]. The resonance peak therefore corresponds to a true collective mode below the continuum, in analogy to the spin waves in Fe or Ni. However, in contrast to the situation in these magnetically ordered systems, the collective mode is not a Goldstone mode that restores a spontaneously broken symmetry. The broken symmetry in a superconductor (electromagnetic gauge symmetry) has nothing to do with the magnetization whose dynamics we are measuring. In this sense, the magnetic mode observed in high temperature superconductors is much more subtle than spin waves in ferromagnetic metals.

A microscopic theory of the spin excitations in copper oxides that starts from a Hamiltonian instead of phenomenological assumptions does not yet exist. There are, however, many indications of a direct relation between the mechanism of high temperature superconductivity and the spin excitations measured by neutron scattering. One approach is the so-called “tunneling spectroscopy” which looks at the spectrum of electrons emitted through the insulating layer of a tunnel junction upon application of a bias voltage. If tunnel spectra contain strong features at the same energies as known collective modes in the superconductor, this is indicative of a strong interaction between the superconducting electrons and these collective modes. In the 1970’s, a match between such features in tunnel spectra and features in the phonon density of states measured by neutron spectroscopy yielded the most unambiguous experimental evidence to-date for a strong electron-phonon interaction and phonon-mediated superconductivity in ordinary metals such as Pb or Al (Fig. 11).

Some researchers have claimed a similar match between features observed in the tunnel spectra of copper oxide superconductors and the magnetic resonant mode observed in the neutron experiments described above. If confirmed, this would be a persuasive indication of a magnetic pairing mechanism. However, this claim is still hotly debated in the copper oxides. For a different strongly correlated metal, UPd<sub>2</sub>Al<sub>3</sub>, the situation is already more clear-cut. This material has *f*-electrons in its valence band, orders antiferromagnetically around 14 K and becomes superconducting at 1.8 K. Neutron scattering has revealed an antiferromagnetic excitation mode around 1 meV with a similar temperature dependence as the “resonant mode” in the high-T<sub>c</sub> materials. A strong feature in the tunnel spectrum of this material at the same energy provides powerful evidence of a spin-fluctuation mediated pairing mechanism (Fig. 11). Detailed work of this type is also the best hope for eventually elucidating the pairing mechanism responsible for the high superconducting transition temperatures in the copper oxides.



Pb phonons



UPd<sub>2</sub>Al<sub>3</sub>  
spin excitation

**Fig. 11:** Tunnel spectrum of a Pb-Al<sub>2</sub>O<sub>3</sub>-UPd<sub>2</sub>Al<sub>3</sub> junction. Al<sub>2</sub>O<sub>3</sub> is an insulator, Pb is a conventional (phonon-mediated) superconductor [7]. The feature at low energy can be matched to a spin fluctuation mode of the unconventional superconductor UPd<sub>2</sub>Al<sub>3</sub> identified independently by neutron scattering.

## 4. Orbital Degeneracy

As already mentioned, the layered structure of the superconducting copper oxides results in an electronic structure in which only one  $d$ -orbital,  $x^2-y^2$ , is relevant. In transition metal compounds with more isotropic, three-dimensional bonding networks, the valence electrons can often choose between different orbitals. The orbital degeneracy is then broken through a spontaneous lattice distortion, the so-called Jahn-Teller effect, which was described in quantitative detail in M. Sigrist's lecture. As the lattice distortions around neighboring transition metal ions in a chemical compound are coupled, the Jahn-Teller effect is *cooperative* and results in long range *orbital order*. This is nicely illustrated in KCuF<sub>3</sub>:

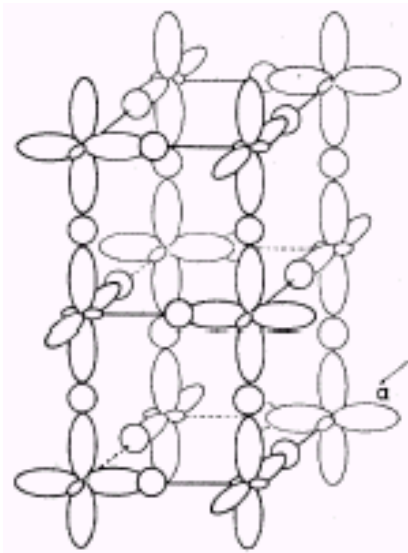


**Fig. 12:** Orbital order in KCuF<sub>3</sub> [8].

Here, Cu is again in the valence state  $2+$ , but the orbital occupied by the Cu hole alternates from site to site due to the cooperative Jahn-Teller effect. Note that there are four short and two long bonds for every copper atom, so that the local symmetry is similar to Fig. 6. The orbital occupations determine the magnetic exchange interactions between the spins of Cu holes on neighboring sites whose signs and magnitudes were summarized in the so-called “Goodenough-Kanamori rules”. As a quantitative treatment was given in M. Sigrist’s lecture, we only summarize a few qualitative aspects in the following sketch:

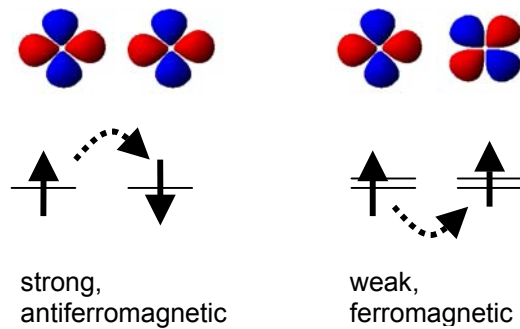


**Fig. 13:** Illustration of one of the “Goodenough-Kanamori rules”: If identical (orthogonal) orbitals are occupied on neighboring lattice sites, the exchange coupling is strong and antiferromagnetic (weak and ferromagnetic).

As a consequence of these rules,  $\text{KCuF}_3$  is an excellent physical realization of a quasi-one-dimensional antiferromagnet, with strong antiferromagnetic exchange interactions along one crystal axis and weak ferromagnetic interactions along the two perpendicular axes.  $\text{KCuF}_3$  is the first real compound in which a “two-spinon continuum” theoretically expected for one-dimensional antiferromagnets was experimentally observed.

A similar example is  $\text{LaMnO}_3$ , another Mott-Hubbard insulator with a nearly cubic lattice structure which contains Mn in its  $3+$  valence state with electron configuration  $3d^4$ . Like  $\text{Cu}^{2+}$ ,  $\text{Mn}^{3+}$  is a Jahn-Teller ion:

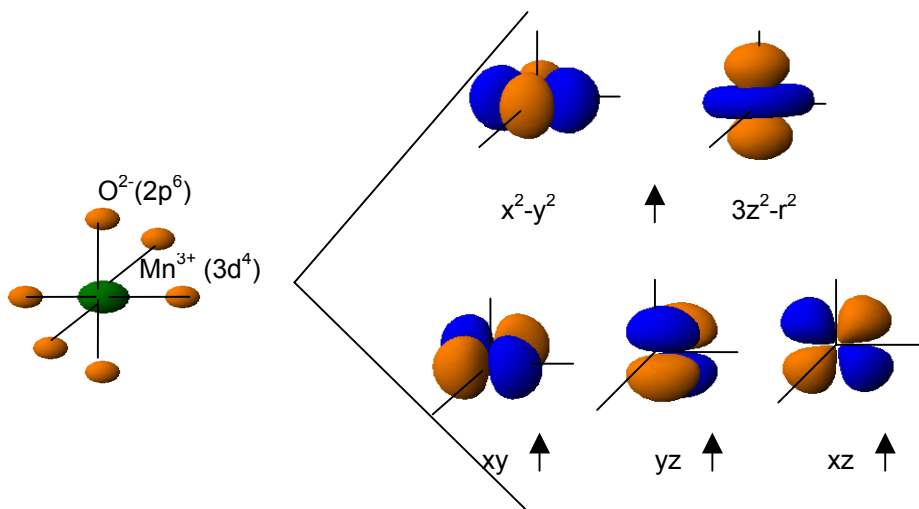


**Fig. 14:** Crystal field splitting of the  $\text{Mn}^{3+}$  ion in an ideally cubic structure. The upper two orbitals are termed “ $e_g$ -orbitals”, the lower two “ $t_{2g}$ -orbitals”. The individual electron spins are aligned due to Hund’s rule; the total spin of the  $\text{Mn}^{3+}$  ion is therefore  $S=2$ . The orbital degeneracy is lifted by the cooperative Jahn-Teller effect.

The cooperative Jahn-Teller effect leads to orbital order at around 800 K, which can be observed in x-ray or neutron diffraction by virtue of the concomitant lattice distortion:

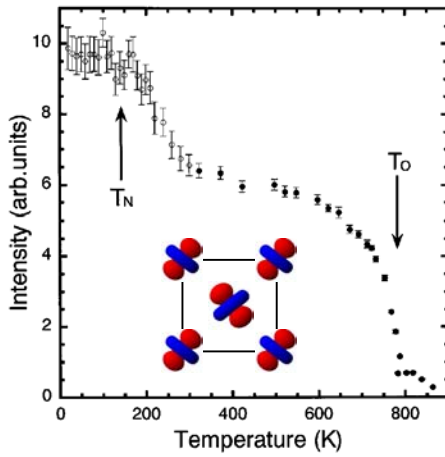


**Fig. 15:** Superstructure reflection characteristic of orbital order in  $\text{LaMnO}_3$  [9]. The inset shows a section of the nearly cubic structure perpendicular to the  $c$ -axis with the orbital ordering pattern. Along the  $c$ -axis (out of the page), identical orbitals are occupied on nearest-neighbor sites.

According to the Goodenough-Kanamori rules, this orbital ordering pattern results in ferromagnetic exchange interactions in a plane perpendicular to the  $c$ -axis, and antiferromagnetic interactions along  $c$ . A magnetic ordering pattern in line with these rules is actually observed by magnetic neutron diffraction at much lower temperature:

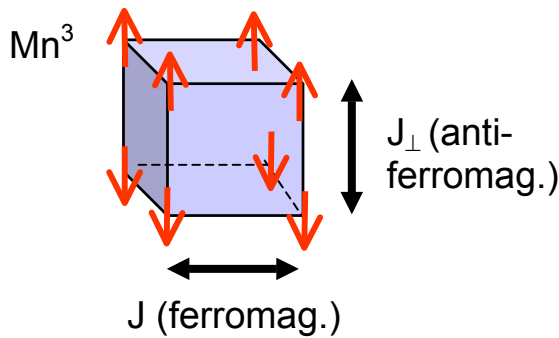


**Fig. 16:** Magnetic structure of insulating  $\text{LaMnO}_3$ .

The spin dynamics in the magnetically ordered state of  $\text{LaMnO}_3$  is therefore highly anisotropic, with ferromagnetic spin wave dispersions along the  $ab$ -plane and an antiferromagnetic dispersion along  $c$ :

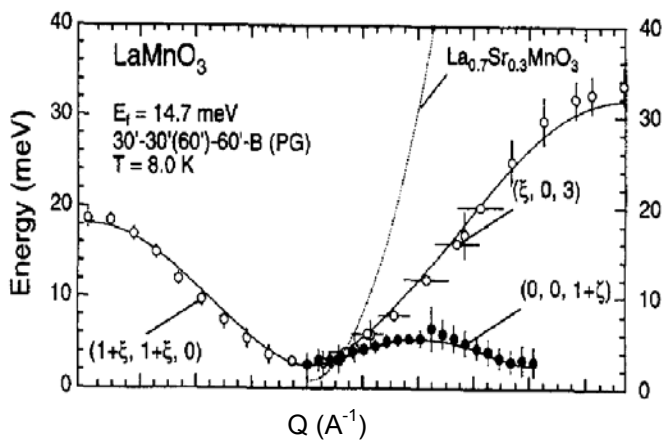


**Fig. 17:** Magnon dispersions in  $\text{LaMnO}_3$  [10].

Like the copper oxides, the manganese oxides can also be doped by chemical substitution. Due to the additional, orbital degree of freedom the resulting phase diagram is considerably more complicated than that of the copper oxides (Fig. 7). The phases realized depend strongly on details of the crystal structure. The phase diagrams of compounds with small Mn-Mn hopping parameters (small conduction band width) tend to contain only Mott insulating states with static ordering patterns in which the Jahn-Teller ion  $\text{Mn}^{3+}$  alternates with the non-Jahn-Teller ion  $\text{Mn}^{4+}$ . These “charged ordered” states are therefore associated with orbital order of a different periodicity than that of insulating  $\text{LaMnO}_3$ . They also exhibit magnetic order and can be thought of as strongly correlated analogs of the charge and spin density waves phases discussed in Section 2 for weakly correlated metals. An example of such a phase diagram is given in Fig. 18.

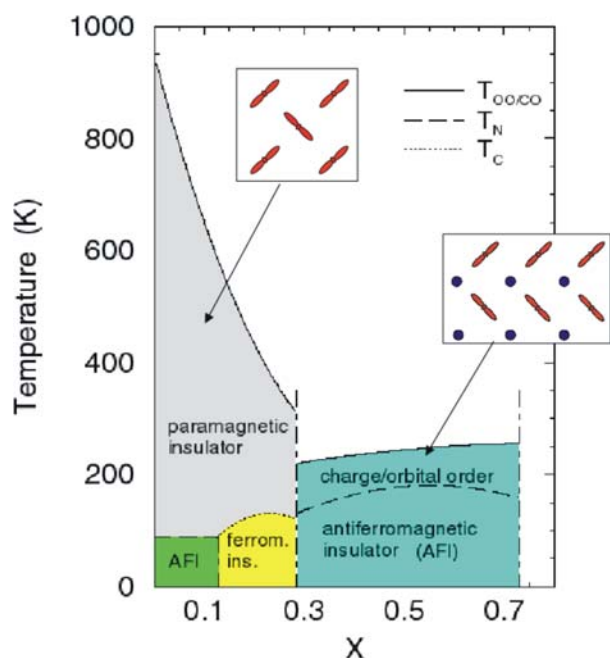


**Fig. 18:** Phase diagram of  $\text{Pr}_{1-x}\text{Ca}_x\text{MnO}_3$ . The  $e_g$ -orbital of  $\text{Mn}^{3+}$  is shown in red, the  $\text{Mn}^{4+}$  ions (with only  $t_{2g}$  electrons) are shown in blue.

Not surprisingly, the spin dynamics in these charge ordered phases is rather complex and it is still a matter of active investigation. Other manganese oxide families with a larger single-electron band width (such as  $\text{La}_{1-x}\text{Sr}_x\text{MnO}_3$ ) exhibit metallic phases as well. The orbital order in these metallic phases is believed to be obliterated by the conduction electrons, which drag the orbitals along with them. Nonetheless, these states tend to be ferromagnetically ordered at low temperatures. The mechanism responsible for ferromagnetic order in metallic manganese oxides, the so-called “double exchange”, is entirely different from the superexchange mechanism discussed above: Ferromagnetic alignment of the  $t_{2g}$  “core spins” ( $S=3/2$ ) on every Mn ion facilitates hopping of the  $e_g$  conduction electrons by virtue of the intra-atomic Hund’s rule, thereby lowering their kinetic energy. Due to the absence of orbital order, the spin dynamics in the metallic phase is exceptionally simple. The anisotropies observed in the orbitally ordered state (Fig. 17) are “washed out” by the orbital fluctuations, and the magnon spectrum becomes perfectly isotropic, that is, it is described by a Heisenberg model with the same ferromagnetic nearest-neighbor exchange coupling in all crystallographic directions:

$$\hbar\omega = 6SJ(1 - \gamma(q))$$

where  $\gamma(\underline{q}) = \frac{1}{3}[\cos(q_x a) + \cos(q_y a) + \cos(q_z a)]$ . An example is given in Fig. 19.

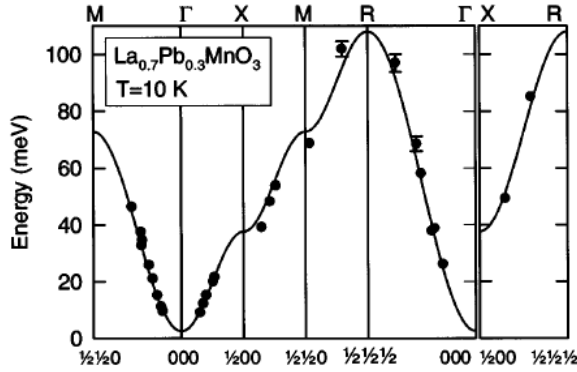


**Fig. 19:** Magnon spectrum of  $\text{La}_{0.7}\text{Pb}_{0.3}\text{MnO}_3$  in its ferromagnetic metallic state. The lines are the result of a fit to an isotropic nearest-neighbor Heisenberg model [11].

Curiously, such perfectly isotropic spin dynamics was also recently observed in *insulating* titanium oxides such as  $\text{LaTiO}_3$  and  $\text{YTiO}_3$  (Fig. 20). These materials have the same nearly cubic crystal structure as  $\text{LaMnO}_3$  and therefore the same crystal field level scheme as in Fig. 14. However,  $\text{Ti}^{3+}$  has only one  $d$ -electron occupying the  $t_{2g}$  manifold, and the orbital degeneracy is hence larger than in the manganates. Moreover, the  $t_{2g}$  orbitals point away from the surrounding oxygen ions so that the coupling to the lattice through the Jahn-Teller effect is substantially weaker. Current theories therefore attribute the isotropic spin dynamics to orbital quantum fluctuations, analogous to those in the metallic manganese oxides. However, in contrast to the manganates, the orbital fluctuations in the titanates are *not* induced by charge fluctuations. Rather, they must be regarded as spontaneous zero-point fluctuations, roughly analogous to the atomic zero-point motion in liquid He. A quantitative description of these orbital quantum fluctuations is currently a matter of active research (see M. Sigrist's lecture).

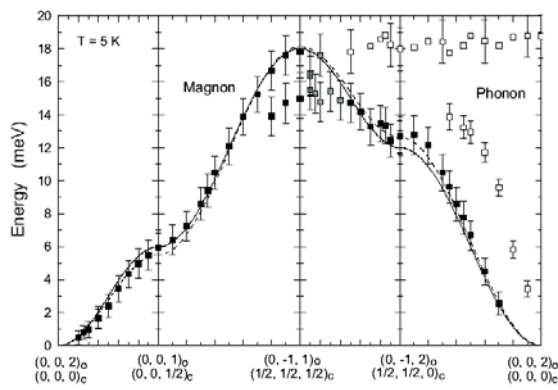


**Fig. 20:** Magnon spectrum of insulating  $\text{YTiO}_3$  in its ferromagnetically ordered state. The lines are the result of a fit to an isotropic nearest-neighbor Heisenberg model [12].

## 5. References

- [1] E. Fawcett, Rev. Mod. Phys. 60, 209 (1988)
- [2] S. Sachdev and J. Ye, Phys. Rev. Lett 69, 2411 (1992)
- [3] B. Keimer et al., Phys. Rev. B 46, 14034 (1992)
- [4] H.F. Fong et al., Phys. Rev. B 54, 6708 (1996); Nature 398, 588 (1999)
- [5] N. Bulut and D.J. Scalapino, Phys. Rev. B 53, 5149 (1996)
- [6] P. Bourges et al., Science 288, 1234 (2000)
- [7] M. Jourdan et al., Nature 398, 47 (1999)
- [8] S.K. Satija et al., Phys. Rev. B 21, 2001 (1980)
- [9] Y. Murakami et al., Phys. Rev. Lett. 81, 582 (1998)
- [10] K. Hirota et al., J. Phys. Soc. Jpn. 65, 3736 (1996)
- [11] T.G. Perring et al., Phys. Rev. Lett. 77, 711 (1996)
- [12] C. Ulrich et al., Phys. Rev. Lett. 89, 167201 (2002); B. Keimer et al., Phys. Rev. Lett. 85, 3946 (2000)